Demonstration of an elliptical plasmonic lens illuminated with radially–like polarized field

Gilad M. Lerman, Avner Yanai, Nissim Ben-Yosef and Uriel Levy*

Department of Applied Physics, The Benin School of Engineering and Computer Science, The Center for Nanoscience and Nanotechnology, The Hebrew University of Jerusalem, Jerusalem, 91904, Israel
** ulevy@cc.huji.ac.il*

Abstract: We demonstrate an elliptically symmetric plasmonic lens that is illuminated by a radially-like polarization field. This illumination function is TM polarized with regard to the plasmonic lens, ensuring optimum coupling of the incident light into surface plasmons polaritons. The structure is analyzed theoretically by using the Green function approach, and a finite difference time domain simulation. Both approaches provide similar results. Specifically we calculate and experimentally measure the field distribution on the surface and a few microns above it. The results show strong dependency of the electric field distribution on the eccentricity of the elliptic structure and the illumination wavelength. The interference of surface plasmons generates a structured pattern consisting of distinct peaks distributed inside the ellipse with locations that are wavelength dependent. This pattern can be used in several applications including structured illumination microscopy, particles beam trapping and sensing.

OCIS codes: (260.5430) Polarization; (240.6680) Surface plasmons.

References and links

1. Z. W. Liu, J. M. Steele, W. Srituravanich, Y. Pikus, C. Sun, and X. Zhang, "Focusing surface plasmons with a plasmonic lens," Nano Lett. **5**(9), 1726–1729 (2005).
2. W. Chen, and Q. Zhan, "Optimal plasmonic focusing with radial polarization," Proc. SPIE **6450**, 64500D (2007).
3. A. Yanai, and U. Levy, "Plasmonic focusing with a coaxial structure illuminated by radially polarized light," Opt. Express **17**(2), 924–932 (2009).
4. A. Yanai, and U. Levy, "The role of short and long range surface plasmons for plasmonic focusing applications," Opt. Express **17**(16), 14270–14280 (2009).
5. G. M. Lerman, A. Yanai, and U. Levy, "Demonstration of nanofocusing by the use of plasmonic lens illuminated with radially polarized light," Nano Lett. **9**(5), 2139–2143 (2009).
6. W. Chen, D. C. Abeysinghe, R. L. Nelson, and Q. Zhan, "Plasmonic lens made of multiple concentric metallic rings under radially polarized illumination," Nano Lett. **9**(12), 4320–4325 (2009).
7. R. Dorn, S. Quabis, and G. Leuchs, "Sharper focus for a radially polarized light beam," Phys. Rev. Lett. **91**(23), 233901 (2003).
8. K. S. Youngworth, and T. G. Brown, "Focusing of high numerical aperture cylindrical-vector beams," Opt. Express **7**(2), 77–87 (2000).
9. U. Levy, C. H. Tsai, L. Pang, and Y. Fainman, "Engineering space-variant inhomogeneous media for polarization control," Opt. Lett. **29**(15), 1718–1720 (2004).
10. I. Richter, P. C. Sun, F. Xu, and Y. Fainman, "Design considerations of form birefringent microstructures," Appl. Opt. **34**(14), 2421–2429 (1995).
11. A. Drezet, A. L. Stepanov, H. Ditlbacher, A. Hohenau, B. Steinberger, F. R. Aussenegg, A. Leitner, and J. R. Krenn, "Surface plasmon propagation in an elliptical corral," Appl. Phys. Lett. **86**(7), 074104 (2005).
12. M. Born, and E. Wolf, Principles of Optics (Pergamon press, 1980).
13. P. M. Morse, and H. Feshbach, Methods of Theoretical Physics, (McGraw-Hill, 1953).
14. S. H. Chang, S. K. Gray, and G. C. Schatz, "Surface plasmon generation and light transmission by isolated nanoholes and arrays of nanoholes in thin metal films," Opt. Express **13**(8), 3150–3165 (2005).
15. L. Schermelleh, P. M. Carlton, S. Haase, L. Shao, L. Winoto, P. Kner, B. Burke, M. C. Cardoso, D. A. Agard, M. G. L. Gustafsson, H. Leonhardt, and J. W. Sedat, "Subdiffraction multicolor imaging of the nuclear periphery with 3D structured illumination microscopy," Science **320**(5881), 1332–1336 (2008).
16. S. Liu, C. J. Chuang, C. W. See, G. Zoriniants, W. L. Barnes, and M. G. Somekh, "Double-grating-structured light microscopy using plasmonic nanoparticle arrays," Opt. Lett. **34**(8), 1255–1257 (2009).
17. G. M. Lerman, and U. Levy, "Tight focusing of space variant vector optical fields with no cylindrical symmetry of polarization," Opt. Lett. **32**, 2194–2196 (2007).

#124312 - $15.00 USD Received 16 Feb 2010; revised 31 Mar 2010; accepted 13 Apr 2010; published 10 May 2010

18. G. M. Lerman, Y. Lilach, and U. Levy, "Demonstration of spatially inhomogeneous vector beams with elliptical symmetry," Opt. Lett. **34**(11), 1669–1671 (2009).
19. P. Lalanne, J. P. Hugonin, and J. C. Rodier, "Theory of surface plasmon generation at nanoslit apertures," Phys. Rev. Lett. **95**(26), 263902 (2005).
20. P. Ginzburg, and M. Orenstein, "Plasmonic transmission lines: from micro to nano scale with λ/4 impedance matching," Opt. Express **15**(11), 6762–6767 (2007).
21. A. F. Oskooi, D. Roundy, M. Ibanescu, P. Bermel, J. D. Joannopoulos, and S. G. Johnson, "MEEP: A flexible free-software package for electromagnetic simulations by the FDTD method," Comput. Phys. Commun. **181**(3), 687–702 (2010).
22. T. Grosjean, and D. Courjon, "Polarization filtering induced by imaging systems: effect on image structure," Phys. Rev. E Stat. Nonlin. Soft Matter Phys. **67**(4), 046611 (2003).
23. L. Aigouy, P. Lalanne, J. P. Hugonin, G. Julié, V. Mathet, and M. Mortier, "Near-field analysis of surface waves launched at nanoslit apertures," Phys. Rev. Lett. **98**(15), 153902 (2007).
24. H. W. Kihm, J. H. Kang, J. S. Kyoung, K. G. Lee, M. A. Seo, and K. J. Ahn, "Separation of surface plasmon polariton from nonconfined cylindrical wave launched from single slits," Appl. Phys. Lett. **94**(14), 141102 (2009).

1. Introduction

In recent years it has been demonstrated that surface plasmons (SPs) can be focused by a plasmonic lens (PL) producing a diffraction limited spot size with an effective numerical aperture (N.A) higher than 1. The high effective N.A is the result of the interference of surface waves having a wavelength smaller than the vacuum wavelength. The basic PL consists of a circular subwavelength slit that is milled into a metal surface. When illuminated, the subwavelength slit converts the incident light into SP waves. These SPs are propagating towards the center of the circle, to form a sharp central spot by the interference of counter propagating SP's. This concept was demonstrated by Liu et. al. [1], where a PL made of Ag layer on top of glass was illuminated by a linearly polarized light and the field distribution was measured by a near field scanning optical microscope (NSOM) and also by recording the intensity pattern in photoresist. Recently, it was suggested and experimentally demonstrated that radially polarized light is a better choice for the illumination of the circular PL instead of a linearly polarized light [2–6]. The unique characteristics of radially polarized light, such as forming a tighter focal spot than linearly polarized light, and a strong Ez component at the focus, have been previously demonstrated [7,8]. Moreover, radially polarized light has another advantage, as it is TM polarized with respect to the annular slit of the PL along its whole circumference. Keeping in mind that TM polarization is required for SP excitation, the radially polarized light is the natural choice for illuminating a circularly symmetric PL. This is in contrast to the case of a linearly polarized light, where its TM component drops as $\cos(\theta)$, where θ is the angle between the polarization direction and the normal to the slit. Therefore, radially polarized light can provide stronger coupling of light into SPs and thus larger enhancement of the field at the focus of the PL can be achieved. In addition, it was shown that radially polarized light illumination allows the constructive interference of the dominant out of plane electric field component (Ez) at the center, whereas linear polarization illumination give rise to the constructive interference of the less dominant in plane electric field component.

Taking this concept one step further, the polarization field distribution can be manipulated to match any slit geometry, such that it will always be TM with respect to the slit, allowing maximal coupling of light into SP. One approach for locally controlling the polarization orientation is the use of space variant subwavelength gratings acting as localized half wave plates which rotate the polarization towards the desired direction at any point across the beam [9,10]. Here we take advantage of this approach to study an elliptical plasmonic lens (EPL), i.e. a subwavelength elliptical slit that is milled into a metal surface (Ag). The EPL is illuminated by a matched polarized beam, i.e. the electric field of the illuminating beam is perpendicular to the slit and therefore can be considered as TM polarized with regard to the ellipse, allowing maximal and equal coupling of light into SPs from every section of the elliptical slit. Although elliptically shaped plasmonic structures have already been demonstrated [1,11], it is the first time where the polarization of the incident beam is matched to this elliptical shape for optimal excitation. For simplicity we define this polarization field as

#124312 - $15.00 USD Received 16 Feb 2010; revised 31 Mar 2010; accepted 13 Apr 2010; published 10 May 2010

"radial-like" polarization. Figure 1 shows a schematic drawing of such an EPL illuminated with a matched polarization field that is always perpendicular to the circumference of the elliptical slit.

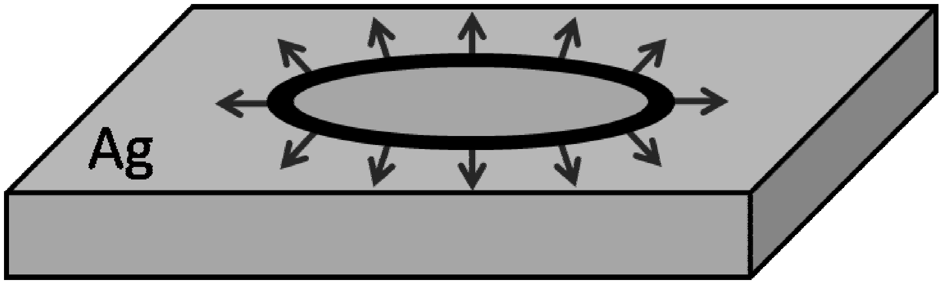

Fig. 1. A schematic drawing of the EPL illuminated with a matched polarization field which is TM polarized with regard to the elliptical slit. The arrows represent the orientation of polarization of the incident light at each point. The Black ellipse represents the slit in the metal.

2. Theoretical and computational analysis

In order to calculate the field distribution within the EPL we used the Green function approach [12] so that

$$U(r) \propto \iint E_{inc}(x', y') \cdot G(|r - r'|) \cdot dx' dy' \tag{1}$$

Where U is the z component of the electric field within the EPL, E_{inc} is the z component of the electric field on the ellipse's circumference, G is the green function of the problem, $|r-r'|$ is the distance between the observation point and the sources located on the slit, and the integration is performed over the ellipse's boundary. The SPs propagate on the metallic surface, i.e. the diffraction problem is two dimensional. Thus, one needs to use the two dimensional green function which is the 0th order Hankel function of the first kind [13,14] $H_0^{(1)} = J_0(k|r-r'|) + iN_0(k|r-r'|)$ where k is the wave number and J_0, N_0 are the 0th order Bessel functions of the first and the second kind, respectively. Assuming that the incident electric field is constant on the slit, we calculate the electric field distribution inside the EPL for the vacuum wavelength of $\lambda_0 = 1064$ nm where the metallic layer is assumed to be perfect. We found that the SP interference pattern strongly depends on the eccentricity of the ellipse, the polarization of the incident light and the wavelength of illumination. The eccentricity of an ellipse is given by $\varepsilon = \sqrt{1-(b^2/a^2)}$, where a and b are the semi major and semi minor axis of the ellipse, respectively. To validate our calculations, we also computed the field propagation through the same structures using finite difference time domain (FDTD) simulation and obtained similar results. Figures 2 a, b and c show the calculated intensity of the z-polarized electric field component $|E_z|^2$ for the case of illuminating an ellipse with eccentricity of 0.6 and a semi major axis of 10 microns, by a radially-like polarized field at wavelengths of λ_0, $0.97\lambda_0$ and $0.9\lambda_0$, respectively. As can be seen, a well-defined structured pattern with distinct peaks distributed inside the EPL is obtained. The exact position of these peaks varies with the wavelength of illumination. The structured pattern may be used for structured illumination microscopy where a high resolution is obtained by gathering additional information from the interaction of the illumination pattern with a specimen that is placed on top of the EPL [15]. Plasmonic structures were recently used for demonstrating the concept of structured illumination microscopy [16]. Further improvement in resolution may be obtained by performing a wavelength scan. The peaks will be shifted across the sample as a function of wavelength, and thus a specimen will be sampled by many different illumination functions, providing an effective super resolution imaging approach.

#124312 - $15.00 USD Received 16 Feb 2010; revised 31 Mar 2010; accepted 13 Apr 2010; published 10 May 2010

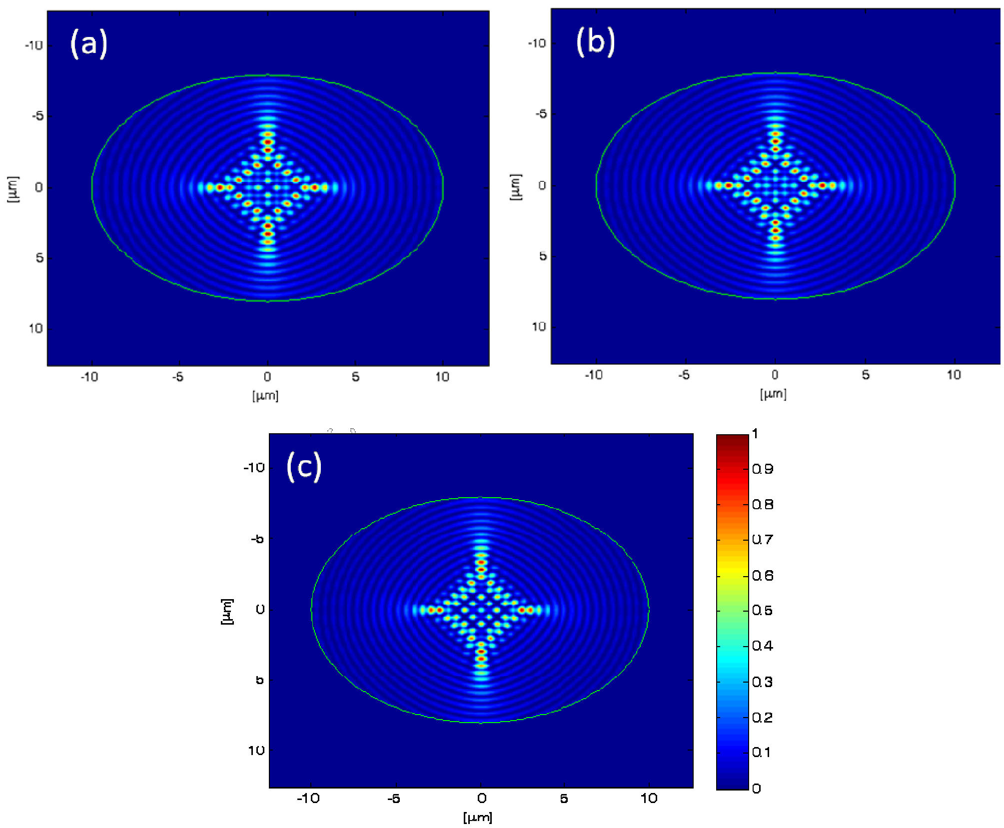

Fig. 2. Normalized $|Ez|^2$ intensity distribution across ellipses with eccentricity of 0.6 and a semi major axis of 10 microns illuminated by a radially-like polarization field with wavelengths of (a) λ_0, (b) $0.97\lambda_0$ and (c) $0.9\lambda_0$, respectively. The scale bar is common to all 3 figures.

Next we compare the calculated patterns with a case where the same EPL is illuminated with a "conventional" linear polarization. The result is shown in Fig. 3. As can be seen, SPs are generated only from sections where the polarization is TM with regard to the slit. Because of this partial symmetry, the obtained interference pattern is smeared across the EPL, and a dark line is obtained at the center of the EPL. This dark line is due to destructive interference of the Ez field at the center and it can be considered as an extension of the dark spot obtained in circular symmetric PL when it is illuminated by a linearly polarized light.

#124312 - $15.00 USD Received 16 Feb 2010; revised 31 Mar 2010; accepted 13 Apr 2010; published 10 May 2010

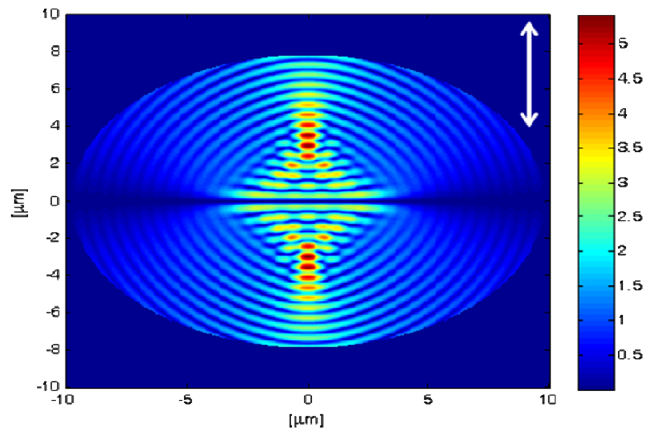

Fig. 3. $|Ez|^2$ intensity component for the case where an ellipse with eccentricity of 0.6 and a semi major axis of 10 microns is illuminated by a linearly polarized light. The incident polarization direction is marked by the white arrow.

3. SPs measurements at the surface of the EPL

Previously [17,18] we designed and generated polarization fields having an elliptical symmetry, by the use of space variant subwavelength grating elements. Having these elements in hand, we fabricated EPLs with eccentricity that matches the eccentricity of the polarization fields. The EPL was fabricated by depositing 200 nm thick Ag layer on top of a glass surface followed by a FIB milling to define a transparent elliptical slit in the metal. The width of the slit was chosen to be 250 nm corresponding to $0.23\lambda_0$ at our wavelength of operation (Nd:YAG laser, λ_0 = 1064). This slit width was found to be ideal for efficiently generating SPPs at the slit edge [19], and for low coupling to radiative modes due to the abrupt termination of the slit [20]. Figure 4 shows a scanning electron micrograph (SEM) of an EPL with an eccentricity of 0.79 and a semi major axis of 10 microns.

The EPL was measured as follows: The linearly polarized light emerging from the laser is converted to the desired polarization field by the subwavelength grating element. After polarization conversion, the beam is focused onto the sample, which is situated on the stage of an inverted microscope, by a 4x objective lens. The sample is raster scanned by a near-field scanning optical microscope (NSOM, Nanonics Imaging Ltd) using a metal coated tapered fiber probe with a circular aperture of 250 nm diameter. The light collected by the probe is guided by the optical fiber and detected by an IR femtowatt photoreceiver. Using the feedback mechanism of the NSOM system the probe is either kept in contact with the sample (tapping mode) or within a constant distance from it (constant height mode).

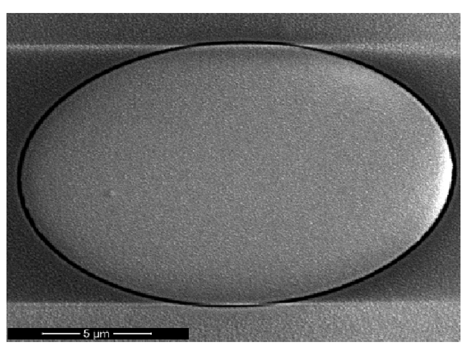

Fig. 4. An SEM picture of an EPL with eccentricity of 0.79 and a semi major axis of 10 microns.

#124312 - $15.00 USD Received 16 Feb 2010; revised 31 Mar 2010; accepted 13 Apr 2010; published 10 May 2010

Figures 5a and b show the NSOM measurement and the computer simulation of the Ez^2 intensity component as generated by an EPL with eccentricity of 0.79 and a semi major axis of 10 microns. The EPL is illuminated by a matched radially-like polarization field. To validate our simulation results and to demonstrate the flow of energy in the EPL, we also calculate the intensity distribution at different time slots using finite difference time domain (FDTD) simulations. In our FDTD model we assume a thin perfect electric conductor layer with an elliptical aperture, excited by the radially-like polarized field. Media 1 shows the evolution of the SPs intensity pattern with time inside the EPL. For our FDTD calculations we use Meep [21], a free software FDTD package.

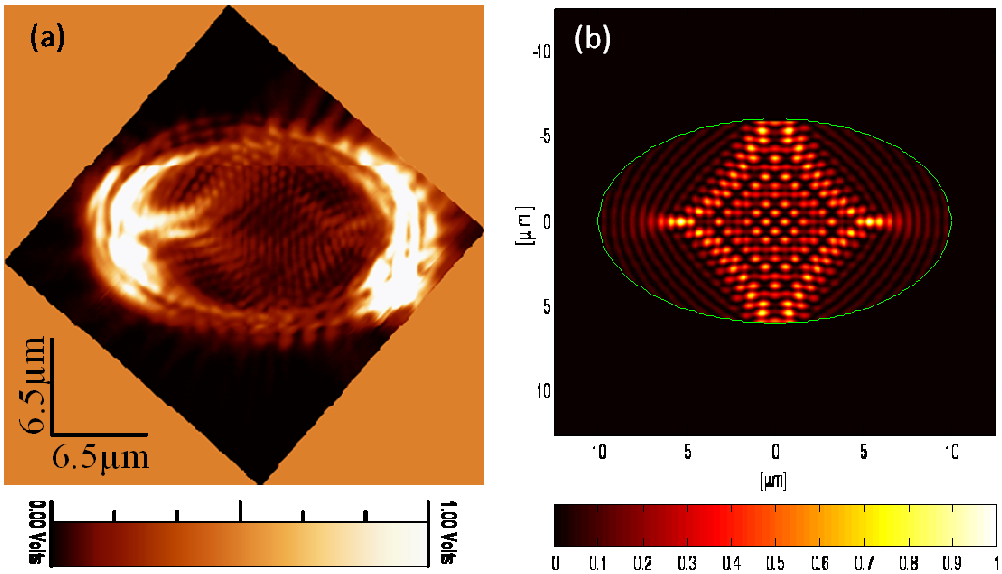

Fig. 5. NSOM measurement (a) and computer simulation (b) of the $|Ez|^2$ intensity component as generated by an EPL with an eccentricity of 0.79 and a semi major axis of 10 microns. The EPL is illuminated by a matched radially-like polarization field. The time evolution of the $|Ez|^2$ intensity component can be seen in (Media 1). This movie is based on finite difference time domain calculation using Meep.

The measured electric field distribution is comparable to our computer simulation, with concentration of energy towards the foci of the ellipse. Nevertheless, the fine details are not in exact agreement and we believe this is because of: 1- Non uniform illumination caused by the imperfect polarization conversion element. 2- Slight misalignment between the polarization field and the EPL. 3 – Defects in the EPL that were developed during the NSOM scan. 4 – The assumption of perfect metal which ignores: A- losses, B – a slight change in the effective index of the SP wave (about 1%) and C - the existence of an in plane electric field component in the measurement. This issue is explained in the next paragraph.

Previous studies showed that the in plane field component couples more efficiently to the apertured NSOM probe compare with the out of plane field component (Ez) [22]. Nevertheless, for SPs, the ratio between Ez and $E_{in\text{-}plane}$ is determined by the dielectric constants of the metal (ε_m) and the dielectric (ε_d), as $|Ez|^2/|E_{in\text{-}plane}|^2 = |\varepsilon_m|/\varepsilon_d$. At our wavelength of operation, the dielectric function of Ag is $\varepsilon = -52 + 3.5i$, thus the ratio $|Ez|^2/|E_{in\text{-}plane}|^2$ is ~52, meaning that despite of the weak coupling of Ez to the probe, the measured intensity is still expected to correspond mostly to $|Ez|^2$. Yet, the strong coupling of the in plane field component may affect the obtained results.

4. Measurements of diffracted waves above the EPL

Next we performed an NSOM measurement few microns above the EPL. In contrast to the previous section, in this regime the SPs can be neglected due to their exponential decay along

#124312 - $15.00 USD Received 16 Feb 2010; revised 31 Mar 2010; accepted 13 Apr 2010; published 10 May 2010

the z axis, and the field distribution is given by the diffraction of waves emanating from the slit. These waves are known as cylindrical waves and have been studied before for other geometries [23,24]. The results of our measurements, alongside our computer simulation are shown in Fig. 6a and b, respectively. The simulations were performed using Meep and show the total energy density of the electric field. Comparing between Figs. 5 and 6 we notice a 90 degrees rotation of the pattern between the two cases. The scan in Fig. 5 was performed on the surface of the EPL – therefore the measurement shows the electric field just near the ellipse's apperture and has the same orientation as the aperture. The scan in Fig. 6, on the other hand, was performed few microns above the EPL where diffraction plays an important role so the orientation of the ellipse is rotated just like the diffraction pattern from an elliptic apperture is rotated by 90 degrees with respect to the aperture.

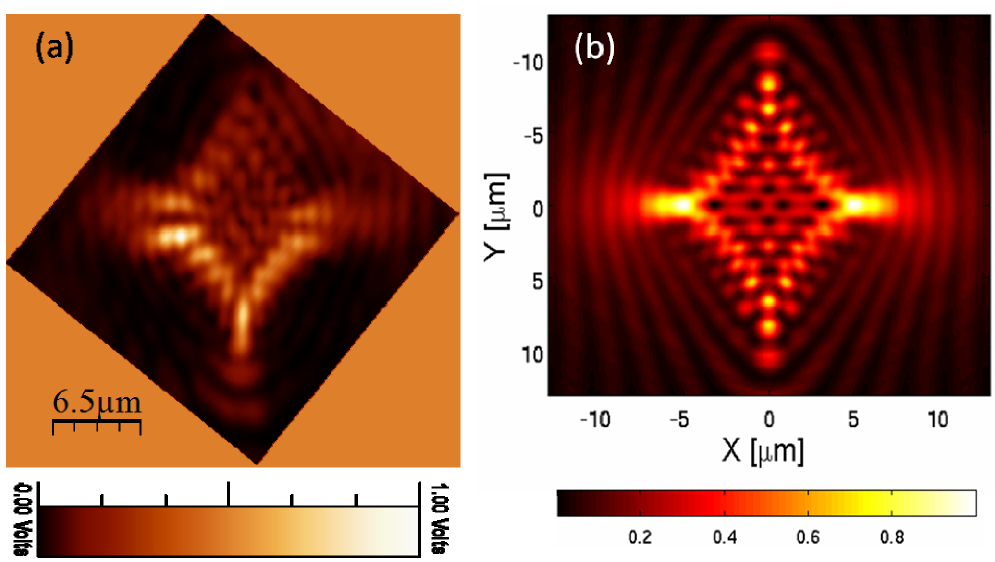

Fig. 6. (a) An NSOM scan performed few microns above the same EPL of Fig. 4. (b) A corresponding computer simulation showing the electric energy density.

5. Conclusions

We demonstrate the concept of polarization field manipulation for efficient coupling of light to plasmonic structures. Specifically, a plasmonic lens with elliptical geometry was illuminated with a matched TM polarized field, generated by the use of subwavelength gratings. The field within the plasmonic lens was measured by NSOM on the metallic surface as well as few microns above it. The experimental results show good agreement with theory revealing a well distinct pattern of SPs inside the elliptical plasmonic lens. This pattern strongly depends on the eccentricity of the ellipse as well as on the illumination wavelength. We believe that the elliptical plasmonic lens can be used in a variety of applications such as structured illumination microscopy, particles beam trapping and sensing.

Acknowledgment

The authors thank Asaf Klein for generating the EPL using the FIB tool, Rami Gabay for his assistance in metal deposition and Yigal Lilach for his assistance in the fabrication of the polarization converter. We acknowledge the financial support of the Israeli Science Foundation, the Israeli Ministry of Science, Culture and Sport and the Peter Brojde Center for Innovative Engineering and Computer Science. G. M. Lerman gratefully acknowledges the support of the Eshkol Fellowship.

#124312 - $15.00 USD Received 16 Feb 2010; revised 31 Mar 2010; accepted 13 Apr 2010; published 10 May 2010